Cargo Ships & Coastal Smog: A Case Study of San Pedro Bay

Philip Economides*

Texas Tech University

November 19, 2024

Abstract

Vessel queuing procedures at maritime ports may induce strategic changes in polluting activities of transport operators. This paper documents a reduction in vessel emissions following the introduction of San Pedro Bay's new ETA-based queuing system. Using geospatial vessel position data in monitored US coastal areas, alongside records of vessel departures at foreign ports of origin, I show that the global emissions of containership voyages servicing Los Angeles and Long Beach declined, on average, by 11.2%. This effect is explained by the added certainty of vessel admittance times, incentivizing ships to slow their voyage speeds and strategically limit local wait times. However, guaranteed queue positions also attracts greater commercial activity, which led to an overall deterioration in local air quality, despite per vessel emissions falling.

JEL Codes: D62, F18, F64, L51, Q52, Q53, R41
Keywords: local environmental policy, transport externalities, local air pollution, port logistics, vessel queues, congestion, maritime trade.

*Department of Economics, Texas Tech University. Contact: peconomi@ttu.edu

I am indebted to Woan Foong Wong, Bruce Blonigen, Anca Cristea, and Nicole Ngo for their advice and guidance. I would like to thank Mark Colas, Grant McDermott, Ed Rubin, as well as seminar participants at the University of Oregon, the Midwest Economic Theory and International Trade Conference, and the AERE@OSWEET online forum for their suggestions and comments. All remaining errors of this initial draft are my own.

1. Introduction

According to the World Bank, international trade in 2022 represented 62 percent of global GDP – a remarkable ascension from a 24 percent share in 1970. With goods more commonly sourced from abroad, the average transportation distance of intermediate and final goods has also grown. From 1965 to 2020, the cargo weight of short-distance trade rose by 45 percent, while longer-distance voyages more than doubled their cargo volumes (Ganapati and Wong, 2023). Given these trends, the maritime shipping industry has developed a significant carbon footprint.[1]

This form of activity – in which 70 percent of maritime emissions occur within 400 km of coasts (Corbett et al., 2007) – contributes to harmful health outcomes for local populations (Capaldo et al., 1999; Liu et al., 2016; Gillingham and Huang, 2021; Zhang et al., 2021). Reducing global shipping emissions presents two challenges; (i) vessel ownership is well distributed across countries, highlighting a need for concerted global governance efforts, and (ii) the available tools for reducing emissions are indirect in nature, which allows for strategic responses by key stakeholders. Since the behavior of households and firms is a key component of plans to decarbonize the transportation sector in the US and elsewhere, the policies of port authorities can be instrumental in shaping behaviour.

This paper uses real-time data on maritime traffic conditions to examine how the introduction of an estimated time of arrival (ETA) based queuing system contributed to maritime decarbonization. I use the case study of San Pedro Bay, which sought to mitigate a large increase in local vessel emissions through this new logistical process. Under the prior system, queue positions at the ports of LA and Long Beach were issued on a first-come first-serve basis upon entering within 25 nautical miles of the San Pedro Bay port complex. Vessel operators' choice of voyage speed influenced their assigned queue position. Should a port be at full capacity, vessels could either drop anchor in close proximity to the cities of Los Angeles and Long Beach or drift nearby, and begin contributing to local port emissions.

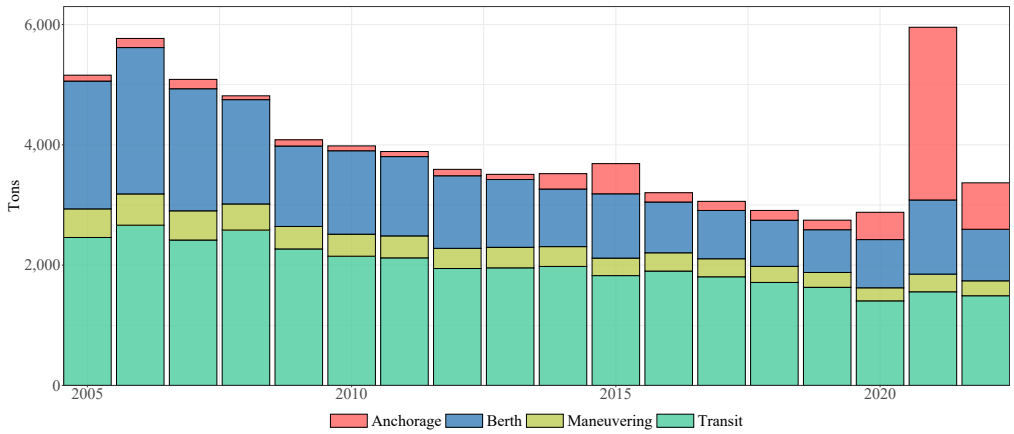
The US economic recovery from the COVID-19 epidemic led to a dramatic increase in import demand, reflected by record numbers of commodity-laden containers entering the US between October 2020 and November 2021.[2] This increase in maritime trade activity caused historic levels of congestion across US ports, leading to prolonged vessel queues and abnormally high GHG emissions. For example, the

[1] Maritime shipping represents 2.89 percent of global CO_2 emissions (IMO, 2021).

[2] 2021 represented an 15.4 percent annual increase in container traffic, as opposed to a long run average of 3.5 percent across the prior decade of activity.

Los Angeles Port Authority's Inventory of Air Emissions (2021) reports a 69 percent annual increase in port emissions of PM_{10} and PM_{25} between 2020 and 2021 – 143 percent specifically for ocean-going vessels. Contributions through the anchorage and queuing stages of vessel operations represented the majority of these emissions (Figure 1) and were driven primarily by containerships (Figure 2). This period of congestion led to numerous cases of environmental damage. In October 2021, just a month prior to policy introduction, a crude oil spill occurred. This was later attributed to anchor damage caused to a nearby pipeline by two containerships, which resulted in losses and clean-up costs worth an estimated 160 million USD.[3]

Figure 1: NOx Emissions (tons), by mode



Source: Los Angeles Port Authority's Inventory of Air Emissions (2021, 2022).

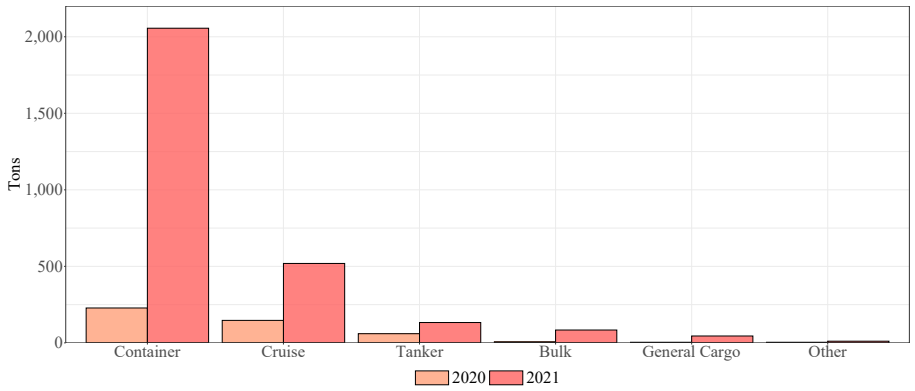
To address the ports' escalating levels of pollution and prevailing environmental damage, the vessel queuing system was updated. On November 11th 2021, the ports of LA and Long Beach jointly announced a new procedure in which vessels would be assigned queue positions by Pacific Maritime Management Services. Rather than the prior "first-come first-serve" process, a queue position would instead be determined by an estimated time of arrival (ETA) from a prior port of departure, assuming a constant travel speed. Furthermore, arriving ships are required to wait outside the 'Safety and Air Quality Area', 150 nautical miles out at sea, rather than within the anchorage zone.

Although the policy may reduce travel speeds through guaranteed queue positions, the added requirement to remain adrift further out at sea introduces an ambiguous global vessel emissions effect. If vessels hardly changed their speeds and fuel consumption while adrift off the continental shelf is particularly taxing on emis-

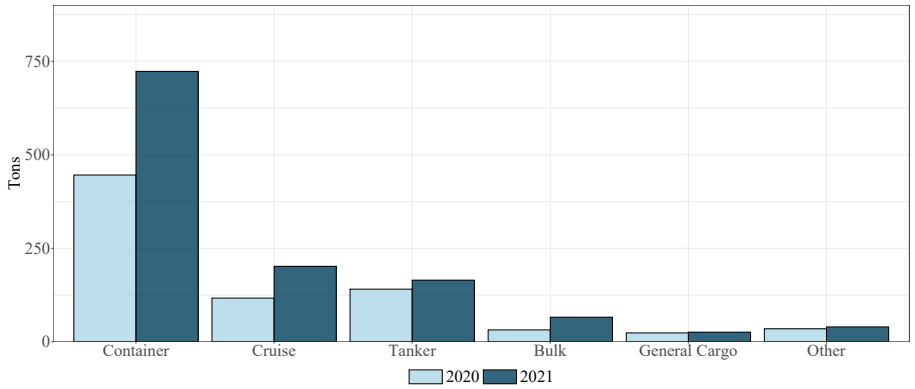
[3]See National Transportation Safety Board, Project Summary: Marine Investigation - 130 Docket Items - DCA22FM001 and Report MIR-24-01, "Anchor Strike of Underwater Pipeline and Eventual Crude Oil Release". Last Accessed 03/09/2024.

Figure 2: NoX Emissions by Vessel Type and Mode

(a) Anchorage



(b) Berth (At Dock)



Source: Los Angeles Port Authority's Inventory of Air Emissions (2021).

sion levels, this policy could be considered a form of environmental NIMBY-ism, similarly to cases featured in Morehouse and Rubin (2021) and Zou (2021).[4] In this case, ports would be reaping the commercial benefits of their property rights while exporting the cost of any resulting air pollution. Alternatively, suppose speed reductions are considerable or vessels spend less time idling due to improved certainty on port admittance. In that case, the greater fuel expended during the queuing process may be negligible in comparison. Under such circumstances, this logistical practice may offer oversight bodies, such as the IMO or DOT, an additional policy tool through which to meet the long-term goals of a decarbonized maritime transport sector.

[4] "Not In My BackYard", a term coined by Mitchell and Carson (1986). Often associated with cases in which a property owner wants a beneficial economic activity to occur on her property while expelling the negative externalities of production elsewhere.

I quantify this policy's local and global effect on vessel-related carbon emissions. First, I use a difference-in-difference approach to estimate the new system's effect on areas in proximity to the ports, using the EPA's local air quality measures, where relevant controls consist of (i) port areas of Oakland, Seattle and Tacoma, and (ii) nearby inland regions.[5] Although prevailing vessel count data suggests a dramatic reduction in local emissions following a decline in ships in anchorage, I find evidence to suggest that the countervailing effects of increased container traffic contributed to an overall decline in local air quality. I also ask whether this decision simply shifted emissions elsewhere or functioned as a tool to reduce global vessel emissions. I resolve this ambiguity by weighing changes in both voyage & queuing behaviour and estimate an 11.2% decline in the global emissions of containerships inbound for San Pedro Bay, due to the new vessel queuing system.

This paper contributes to several strands of literature. Firstly, it adds to studies leveraging use of relatively modern transportation data (Heiland et al., 2019; Prochazka et al., 2019; Tumbarello et al., 2019; Brancaccio et al., 2020; Wong, 2022; Wong and Fuchs, 2022; Molina et al., 2024). As Klotz and Berazneva (2022) highlights, the precision of AIS data allows for granular analysis of coastal movements and berthing at local ports, which is essential for estimating associated emissions levels. I rely on automatic identification system (AIS) vessel traffic to observe the exact geospatial positions of vessels at a one-minute resolution through big data queries. The use of this data extends to understanding vessel noise pollution from international shipping lanes too (Scott and Mayer, 2023). I consider vessel-specific, within-route emissions across two stages of vessel transit; (i) voyage – transit between a prior port of departure and US waters, and (ii) queuing – the anchoring and drifting of vessels awaiting port entrance along the US west coast. This study offers a new methodology by which AIS vessel positions can be used to map drifting and anchoring behaviour within port queues and infer individual emission levels across vessels.

I also contribute to topics of transport policy, congestion and environmental conservation (Kinney et al., 2011; Cristea et al., 2013; Ngo et al., 2015; Shapiro, 2016; Rivera, 2021). Gillingham and Huang (2021) finds that at-berth emissions in US ports contributed to reduced childbirth weights. Similarly, Hansen-Lewis and Marcus (2022) concludes that the introduction of US maritime emissions control areas significantly decreased fine particulate matter, low birth weight, and infant mortality. However, strategic responses of transport operators limited these gains

[5]This data has previously been used to highlight how local vessel emissions contribute negatively to health outcomes (Gillingham and Huang, 2021; Hansen-Lewis and Marcus, 2022).

by 50%. I quantify local vessel emissions through queuing activities and quantify global emissions associated with inbound voyages & out-of-port congestion. By holding service lanes fixed across my sample – I mitigate the influence of various strategic responses that transport operators may be availing of. I also document that queuing behaviour, while limited to narrow geographic regions, represents at least 20% of transit time for inbound containerships along the US West Coast.

Third and lastly, this paper advances our knowledge of viable tools for environmental regulatory intervention. Both the International Maritime Organization (IMO) and US Department of Transportation (DOT) have pursued policy seeking to decarbonize ports and the maritime transport sector. For example, the IMO currently targets a reduction in total greenhouse gas (GHG) emissions of maritime transport by 20–30 percent as of 2030 and 70–80 percent by 2040. A recent preview of the "US National Blueprint for Transportation Decarbonization" by the DOT outlines plans to accelerate the transition to clean options in maritime shipping through zero-emission fuels, technologies, energies, and new vessels.[6] I add to the policymaker toolkit by evaluating how low-cost adjustments in queuing procedures could reduce maritime emissions. Given that an ETA-based policy resulted in global emissions falling and vessels spending less time idling outside of harbor regions, this may not only limit negative externalities associated with the industry but also boost its productivity. My findings suggest that queuing activity has acted as the main driver of emission reductions. Small– to medium-sized ports, less subject to excessive queuing behaviour, may be less likely to capture the environmental benefits of this logistical practice.

The remainder of the paper proceeds as follows. Section 2 describes the data before outlining a maritime emissions estimation methodology for the voyage and queuing stages of individual vessel transits. Section 3 details the empirical strategy for identifying the policy effects of the new queuing system and discusses its impacts on maritime emissions, port commerce, and local air quality. Section 4 concludes.

2. Data & Inference

In this section, I describe the combination of several publicly available datasets and privately purchased port call data, which allows for the construction of individual vessel emission records between November 2019 to November 2022. The data fall into three broad categories: air quality, vessel, and geographic data. I then outline

[6] Available at https://www.transportation.gov/priorities/climate-and-sustainability/us-national-blueprint-transportation-decarbonization. Last accessed on May 30th 2024.

how I infer associated fuel consumption and emission levels using observed vessel–voyage events. I elaborate on data preparation in Appendix A3, Section I.

2.1. Data

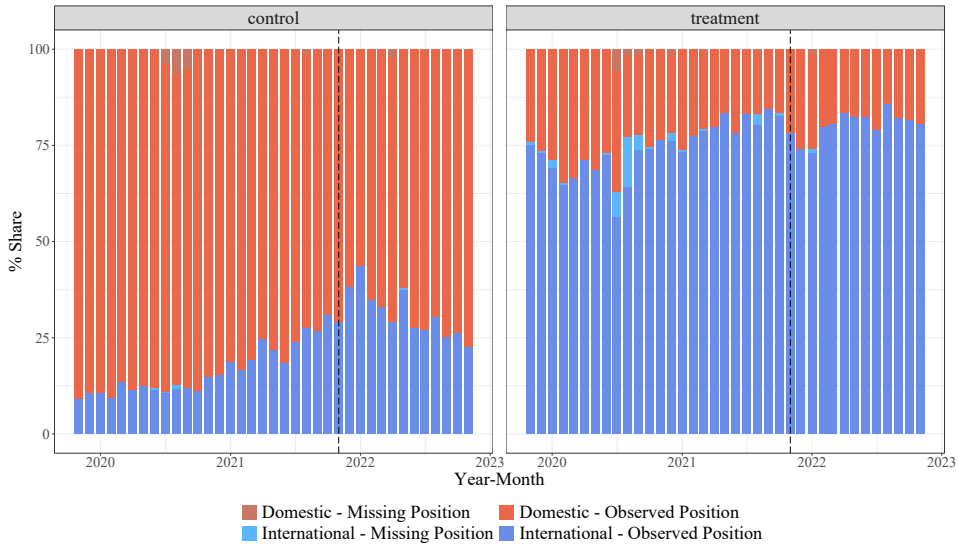
Vessel movements: I have purchased port call data from MarineTraffic (MT), which provides a record of port entrances and exits internationally. I focus on a subset of visits across the US west coast – Seattle, Tacoma, Oakland, Los Angeles and Long Beach – dated between November 2019 and November 2022. MT data details each vessel's prior port of departure and departure time, and port of arrival and arrival time. Each vessel is also uniquely identified by their assigned International Maritime Organization (IMO) codes, which remain invariant to changes in ownership, flag and vessel name. Upon cleaning, this dataset consists of 1,061 uniquely identified vessels servicing 10,035 port visits, where vessels' container capacities range from 200–23,000 twenty-foot equivalent units.

Port call data reveals transit routes, distances, and travel speed, but does not allow one to distinguish between voyage and queuing stages of transit. I combine MT with records of individual vessel movements in US waters to distinguish between these separate stages. These US Coast Guard records use vessels' transceivers that signal the IMO code, status, speed, geo-location, and name of a given ship. I use a publicly available provision of this signal data from MarineCadastre (MC) for containership vessel movements at a minute resolution between January 2019 to December 2022. Lastly, I use time-invariant vessel characteristics from VesselTracking (VT) to assign each vessel their gross size and container capacity. These metrics are key in interpreting how vessel speed maps into fuel consumption.

Using unique vessel IMO codes and associated transit timelines, I combine the coordinates and timestamps of vessels' MT port departures with MC reappearances in US waters. This allows for the assignment of exact travel distances and speed to each individual vessel voyage stage. Transit between US waters arrival and eventual admittance into a US port represents the queuing stage of each voyage. Combining these two events represents the full transit experience of an individual vessel. By joining the two datasets, I can discern which transits in US waters represent international journeys (Figure 3).

Upon dropping extreme outliers – determined based on average travel speeds of individual voyages – I use a sample of 10,035 vessel voyages serviced by 1,061

Figure 3: Match Status by Origin and Group



distinct containerships.[7] Table 1 characterize each included port by period.

Table 1: Summary Statistics of Vessel Voyages

Port	Period	Visits	Vessel Age	Max TEU	Dwell Time	Voyage Time	Voyage Speed
Long Beach	pre-	1708	11.45	7705.59	93.97	237.38	17.22
Long Beach	post-	751	12.74	7466.68	100.84	339.94	15.12
Los Angeles	pre-	1890	10.94	7491.60	119.64	259.50	18.22
Los Angeles	post-	800	11.27	7310.79	132.11	385.55	14.62
Oakland	pre-	1906	12.84	7145.26	48.77	36.09	4.01
Oakland	post-	729	16.06	5370.96	67.75	124.45	6.81
Seattle	pre-	706	12.68	6341.05	56.10	75.57	5.60
Seattle	post-	375	13.28	5541.22	52.30	196.03	9.29
Tacoma	pre-	936	18.35	4716.93	49.22	150.26	15.30
Tacoma	post-	412	20.64	4721.33	64.44	172.31	14.72

Columns 4–8 report averages across vessels for their respective port and time period. "Pre-" is defined as prior to November 11th 2021, when the new San Pedro Bay queuing system was announced for LA and Long Beach. 'Vessel Age' is reported in years. 'Max TEU' reports the container capacity of vessels, 'Dwell Time' reports the average hours vessels spend handling goods at port. 'Voyage Time' details hours between a departure time and the point at which a vessel reappears in US waters. 'Voyage Speed' is reported in nautical miles per hour.

As these statistics highlight, there are a considerable number of journeys taking place within proximity to the North American continent. Many cases involve vessels completing subsequent visits at nearby ports upon arriving at the US West Coast. For my empirical approach, I first consider the new queuing system's effect on broader vessel activity, and then limit my evaluations to consider only international journeys.

[7] I follow Davies and Jeppesen (2015), which labels extreme outliers as values outside a specific closed range. The lower bound is the 25th percentile of average travel speeds less three times the interquartile range (75th percentile value less the 25th percentile value). The upper bound is the 75th percentile of average travel speeds plus three times the interquartile range.

There is also the potential that transport operators may strategically respond to the policy by switching destination ports from abroad. For example, if I wished to preserve my ability to endogenously influence queue positions, I could elect to switch my initial US entry point to a non-treated port. Upon originating from the non-treated port, my subsequent journey to a treated port has now been reduced dramatically and a far lower percentage of overall transit services is exposed to the new queuing system. To avoid this issue of partial selection out of treatment, I focus my third set of results on the subsample of vessels that maintained services to their original pre-policy destinations after the implementation of the policy. Any vessels that no longer serviced the West Coast, as well as newly introduced vessels appearing only after policy implementation are also excluded to avoid concerns of strategic responses that rotate vessels in and out of the West Coast trade network. "Switcher", "Entrant" and "Exit" vessels are excluded from this third empirical approach. The remaining balanced panel of vessel activity occurring consistently prior– and post-policy includes 2,354 port visits serviced by 301 distinct vessels.

Geographic: I use Port Statistical Area data, made available through the United States Army Corp of Engineers (USACE). After some modifications, this allows me to represent polygon regions of key port areas. Using these boundaries, I identify the exact minute at which port entrances and departures occur across US ports, which spells the end of the queuing stage for a given vessel.

Maritime Commerce: I measure commercial activity at a given port based on the number of container units it handles and total containerized trade. For container unit flows, I refer to the bilateral monthly container traffic panel data I gathered individually from ports through a combination of direct requests and FOIAs. This includes inflows and outflows of both loaded and empty container units and the full sample represents over 80 percent of the national throughput of shipping containers for the US (Economides, 2024). USA Trade Online provides the value and volume of bilateral containerized trade flows at the US port level for a given year-month. I subset both of these datasets to reflect the trade and traffic flows of containerized commerce for the ports of Los Angeles, Long Beach, Seattle, Tacoma, and Oakland.

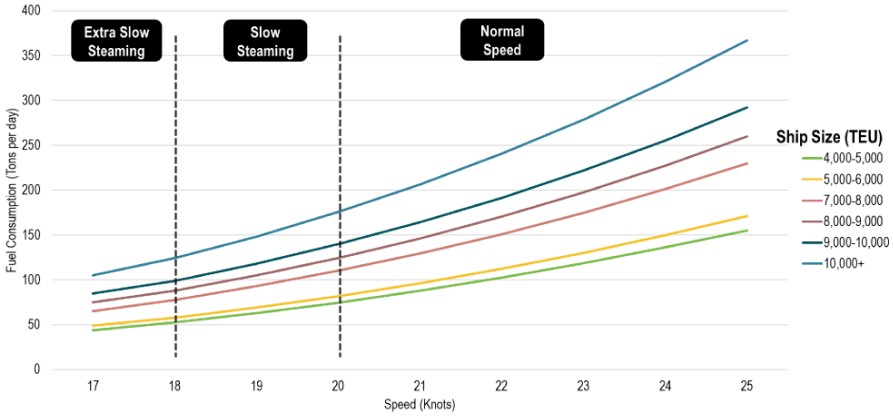
Air Quality: To address emissions associated with the broad set of local sources, including vessel contributions, I use daily Air Quality Index measures provided by the Environmental Protection Agency (AQI). This data relies on outdoor monitors positioned across the US West Coast. States determine monitor placements based on areas of relatively high population. According to the EPA, each state is responsible for developing its own monitoring plan, which is then reviewed and revised every

five years. To include additional monitors, these instruments must follow "stringent siting and quality assurance criteria and are maintained by state and local agencies." Each monitor's report details ozone, particulate matter, carbon monoxide, sulfur dioxide and nitrogen dioxide levels. Each state-county in the dataset contains multiple site locations. I form separate sets of inland and coastal sites across Los Angeles and Long Beach to compare control and treatment group outcomes, respectively. For robustness, I also use comparable zones in proximity to port regions along the West Coast, untreated by the new ETA–based queuing system.

2.2. Fuel Consumption

To study variation in vessel emissions I require a measure of fuel consumption, inferred by inputting vessels' travel speeds and ship sizes (TEU capacity) into fuel consumption functions featured in Figure 4 from Rodrigue (2020).[8] I interpolate across TEU-specific functions and generate a polynomial function using OLS.[9]

Figure 4: Fuel Consumption by Speed and TEU Capacity



Source: Rodrigue (2020). The Geography of Transport Systems, Chapter 4, Transportation and Energy.

Upon calculating fuel consumption for each stage of transit, I use assumptions detailed in the proceeding subsection to generate associated emissions levels for each vessel's various stages of transit.

[8] I do not observe engine types across vessels necessary to use a naval engineering approach featured in Corbett et al. (2009) and Lugovskyy et al. (2023). Ship size suffices in applied studies of vessel emissions (Walsh and Bows, 2012).

[9] Assessing the model fit of this exercise, the function best-behaves at standard cruising speeds of 10–25 knots per hour. However, at slower speeds, inferred functions of fuel consumption levels are unreliable. I introduce a conditional estimation of fuel consumption in which levels below cruise speed (10 knots) receive additional adjustments based on prevailing studies of vessel emissions at slow movement stages. See Appendix A3 (II.) for further details.

2.3. Vessel Emissions

I refer to conversion rates provided by Czermański et al. (2021), which converts tons of fuel to CO_2, SO_X, NO_X, and $PM_{2.5}$ kilogram emissions. I assume vessels are complying with IMO 2020, which mandates an upper limit of 0.5% sulfur content in vessel fuel sources and therefore exclusively use the first row of featured conversion rates (Table 2).

Table 2: Emissivity Indices for Selected Marine Fuels

		[kg/t of Fuel]		
Fuel	CO_2	SO_X	NO_X	$PM_{2.5}$
MDO 0.5%	3206.00	10.50	50.50	2.30
HFO 1.5%	3114.00	31.50	51.00	3.40
HFO 2.0%	3114.00	42.00	51.00	3.40
HFO 3.5%	3114.00	71.50	51.00	3.40
LSHFO 0.5%	3151.00	10.50	51.00	2.30
LSMGO 0.1%	3151.00	2.10	50.50	2.30
LNG	2750.00	¡0.02	8.40	0.02
Methanol	1375.00	0.00	26.10	0.02
HFO + SCRUBBER + SCR	3176.00	0.84	7.65	0.51

Source: Czermański et al. (2021), based on the assumptions of the Med Atlantic Ecobonus (MAE) Project, MAE External Cost Calculator Tool.

For a full set of details regarding how vessel emissions are calculated for slow travel speeds in the local port area, see section III of the appendix.

3. Empirical Strategy & Results

Local emissions associated with vessel movements can be captured through the estimated fuel consumption of containerships reporting AIS signals in the San Pedro Bay area. Combined with global movement data, I dissect individual vessel voyages across voyage, queuing, and berthing stages of transit. In the proceeding section, I first detail my empirical strategy using each segment of transit and then yield policy effects for both local and global vessel emissions. I follow these direct vessel effect findings with broader insights into overall emission level changes for the local port region, relative to other US coastal and nearby in-land control groups.

3.1. Empirical Strategy

Vessel position data reports the speed and status codes of each vessel in US waters, signalling whether vessels are underway (U), maneuvering (M), at anchor (A) or at

berth unloading their goods (B). Using local emissions efficiency – represented by emissions per hour $\left(\frac{e^L_{ipt}}{h^L_{ipt}}\right)$ – summed across these four local transit stages,

$$\frac{e^{\mathrm{L}}_{ipt}}{h^{\mathrm{L}}_{ipt}} = \frac{e^{\mathrm{U}}_{ipt} + e^{\mathrm{M}}_{ipt} + e^{\mathrm{A}}_{ipt} + e^{\mathrm{B}}_{ipt}}{h^{\mathrm{U}}_{ipt} + h^{\mathrm{M}}_{ipt} + h^{\mathrm{A}}_{ipt} + h^{\mathrm{B}}_{ipt}}, \tag{1}$$

I can represent each stage of local activity. For simplicity, I combine activity across underway, maneuvering, and anchoring and refer to it as the "Queuing Stage" (Q), which excludes berthing.

To measure global emissions, I take these measures jointly with voyage (V) emissions of each ship from their respective ports of departure, e^V_{ipt}. The fuel efficiency of each global voyage is expressed as,

$$\frac{e^{\mathrm{G}}_{ipt}}{h^{\mathrm{G}}_{ipt}} = \frac{e^{\mathrm{V}}_{ipt} + e^{\mathrm{Q}}_{ipt}}{h^{\mathrm{V}}_{ipt} + h^{\mathrm{Q}}_{ipt}} \tag{2}$$

To exploit the quasi-experimental nature of this policy change – announced and introduced within a 5-day window – I consider the following specification:

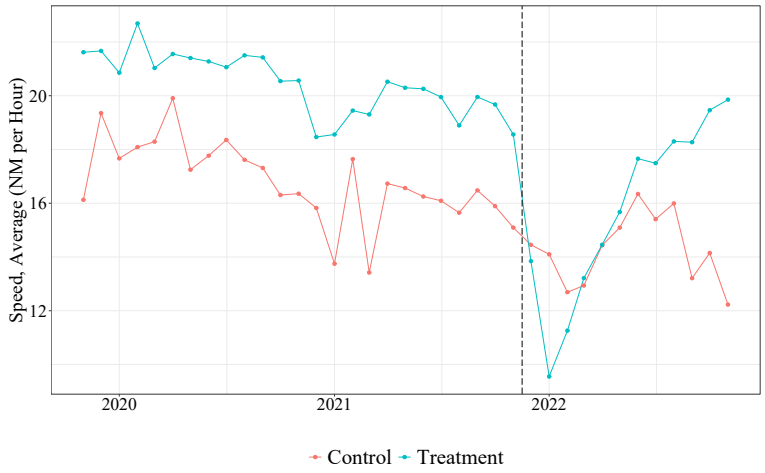
$$Y^S_{iodt} = +\delta^S_1 T_d + \delta^S_2 D_t + \delta^S_3 \left(T_d \times D_t\right) + \phi^S_{io} + \phi^S_t + \mu_{irpt}, \tag{3}$$

where i identifies the individual vessel, io indicates the vessel–voyage route serviced repeatedly over time, and t represents the associated calendar date. Dummies T_d and D_t act as treatment and post-period dummies, respectively.[10] The fuel efficiency outcome variable, Y^L_{ipt}, is emissions-per-hour on a given transit stage, $S \in \{\mathrm{V}, \mathrm{Q}, \mathrm{G}\}$ and can be decoupled for any particular stage of service within a given vessel-voyage, $iodt$. The coefficient of interest, δ^G_3, indicates the global emissions effect of the policy, where $\hat{\delta}^G_3 < 0$ would suggest that this new queue system is a tool that could assist in efforts to decarbonize vessels servicing US ports. Key to this identification approach is the assumption of parallel trends. In Figure 5, I observe parallel trends in vessel voyage speeds in the absence of treatment between treated and control port groups. While the control trend persists, ports of interest experience a sudden slowdown in voyage speeds which coincides with the policy implementation timing.

This suggests that the guaranteed queuing position issued in the post-period portion of the sample may have encouraged a relatively higher percentage of vessels

[10] Control group ports include Oakland, Seattle, and Tacoma which are also exposed to shocks common across the US West Coast, while not treated by this particular policy. The post-period is defined as dates t after November 16th 2021, at which point policy was both announced and implemented.

Figure 5: Parallel Trends in Average Voyage Speeds



to slow-steam towards their West Coast destination, lowering average emission levels across the voyage length of a given transport service. Referring to Eq. (2), this would suggest that $\frac{e^V_{ipt}}{h^V_{ipt}}$ should decline. Furthermore, if a queue position is known then transport operators would be able to better time their arrivals and minimize unproductive idling near the port area.

The increased extent to which vessels must remain idle outside of the treated ports' respective anchorage zones may undermine this local effect through greater degrees of drifting and repositioning. Examining Eq. (2), this would suggest that $\frac{e^Q_{ipt}}{h^Q_{ipt}}$ could rise. This leads to an ambiguity in the values of $\{\delta^G_3, \delta^Q_3\}$, leading to potential doubts over the environmentally-friendly aspect of this logistical change. Should $\hat{\delta}^G_3 < 0$ hold, this would suggest that a simple queuing system change could add to existing efforts by the IMO to reduce the carbon footprint of the maritime transport sector. If $\hat{\delta}^G_3 >= 0$, this would imply that the policy is ineffective in achieving air quality improvements and may inadvertently act as a negative externality generating form of environmental NIMBY-ism. In the proceeding section, I use vessel movement data to isolate the local and global effects of the policy on vessel emissions and mitigate any local confounding factors concerns using Equation (3).

3.2. Voyage Emission Effects

Table 3 details the effect of the new queue system on vessel voyage speeds. Column 3 excludes individual vessels that may have switched ports as a result of the implementation of this policy and acts as the main set of results. This restricts strategic responses across vessel operators that otherwise potentially biases results in columns

1 and 2 (Klotz and Berazneva, 2022). I find that the introduction of this new queue system lowered travel speeds by 16.97%.

Table 3: Difference-in-Difference Estimates – Voyage Speed

	Nautical Miles Per Hour		
	(1)	(2)	(3)
Post–Policy	0.2206***	0.1828**	0.2400***
	(0.0595)	(0.0776)	(0.0909)
Treatment	0.0796***	0.0414*	0.1080
	(0.0256)	(0.0244)	(0.1013)
DiD	-0.2129***	-0.1540***	-0.1860***
	(0.0321)	(0.0373)	(0.0394)
Vessel–Voyage FE	✓	✓	✓
Year–Month FE	✓	✓	✓
Observations	7,055	5,665	2,354
Average Speed, Pre-Policy	18.98	19.14	19.65
R^2	0.82	0.71	0.63

Note: ***: 0.01, **: 0.05, *: 0.1. Standard-errors are robust to clustering within vessel–voyage lanes of transport service. Each observation is a distinct voyage arriving on the US west coast between Nov 2019 and Nov 2022. Column 1 reports the broad diff-in-diff treatment effect on vessels. Column 2 excludes transshipping activity – short subsequent journeys between US ports after their initial arrival from a foreign port of origin. Column 3 only includes Column 2 vessel voyages that maintained the same international trade routes pre- and post- policy. Each regression uses a logged dependent variable. To limit extreme outlier distortions, I exclude any voyages with travel speeds less than the 25th percentile minus three times the interquartile range (75th percentile - 25th percentile) or higher than the 75th percentile plus three times the interquartile range (Davies and Jeppesen, 2015). "Average Speed, Pre-Policy" refers average vessel voyage travel speed of treated US ports prior to 11/11/2021.

Using each vessel's voyage speed and their respective mass, I generate a set of emissions across individual vessel-voyages servicing the US west coast. As displayed in Table 4, my preferred subsample of international voyages yields a 10.47% reduction in total emissions following the introduction of the new queue system. Furthermore, per hour and per nautical mile emissions fell by 25.12 and 9.83 percent, respectively.[11] Although I refer to CO_2 emissions in my findings, the linear relationship prescribed by Czermański et al. (2021) between fuel use and emissivity implies that log changes will be identical across all emission types.

I use an event study design to examine whether these policy effects are permanent or transitive in nature and subset for international journeys that continued maintaining the same service lines following the introduction of the policy. Relative to October 2021, vessels temporarily slow their transit speeds across voyages. As displayed in Figure 6, the two-way fixed effects findings suggests that reduced travel speed adjustments eased off by September 2023.

Similarly, emissions across voyages do see a level reduction that shows mean-reversion behaviour after July 2022. These short–lived effects suggest that an ETA-

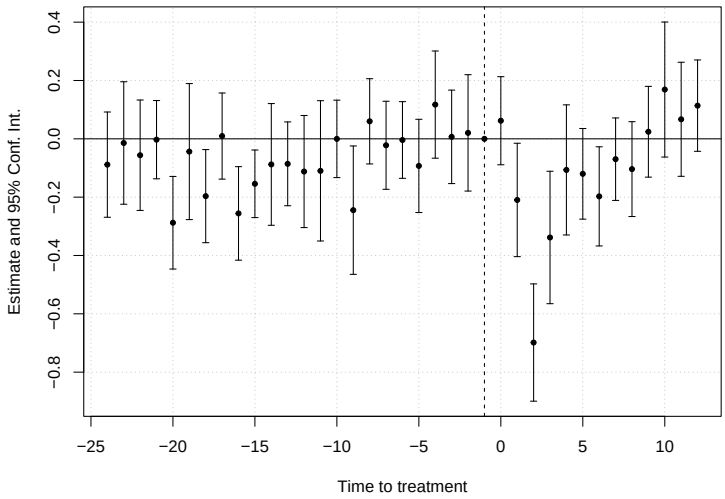
[11]Relaxing the sample to consider all 5,628 international vessel visits yield similar results.

Table 4: Difference-in-Difference Estimates – Voyage Emissions

	CO_2 Emissions			Em. per Hour	Em. per Knot
	(1)	(2)	(3)	(4)	(5)
Post–Policy	0.2929	-0.0503	-0.0895	0.1153	-0.1246
	(0.2917)	(0.0797)	(0.0996)	(0.1422)	(0.0867)
Treatment	1.929***	0.0918**	0.1193	0.1984	0.0900
	(0.3091)	(0.0363)	(0.0823)	(0.1760)	(0.0762)
DiD	-1.159***	-0.1053**	-0.1107**	-0.2894***	-0.1035**
	(0.1411)	(0.0430)	(0.0536)	(0.0777)	(0.0457)
Vessel–Voyage FE	Yes	Yes	Yes	Yes	Yes
Year–Month FE	Yes	Yes	Yes	Yes	Yes
Observations	10,004	5,628	2,346	2,346	2,346
R^2	0.91	0.95	0.91	0.75	0.83

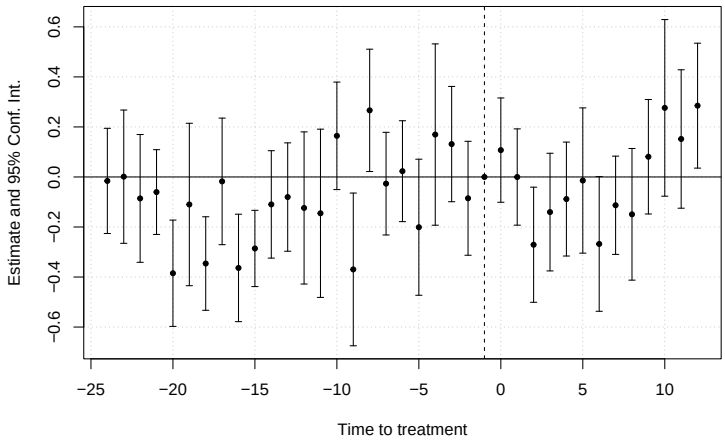
Note: ***: 0.01, **: 0.05, *: 0.1. Standard-errors are robust to clustering within vessel–voyage lanes of transport service. Each observation is a distinct voyage arriving on the US west coast between Nov 2019 and Nov 2022. Column 1 reports the broad diff-in-diff treatment effect on vessels. Column 2 excludes transshipping activity – short subsequent journeys between US ports after their initial arrival from a foreign port of origin. Column 3 only includes Column 2 vessel voyages that maintained the same international trade routes pre- and post- policy. Columns 4 and 5 shift focus to per hour and per nautical mile measures of emissivity, respectively. Each regression uses a logged dependent variable. To limit extreme outlier distortions, I exclude any voyages with hourly emissions less than the 25th percentile minus three times the interquartile range (75th percentile - 25th percentile) or higher than the 75th percentile plus three times the interquartile range (Davies and Jeppesen, 2015).

Figure 6: Event Study (TWFE) - Voyage Speed



based queuing system may not yield substantial boons to the port's efforts to decarbonize long-distance maritime shipping. However, in the next section I shift focus to the queuing leg of transit and demonstrate a substantial reduction in local vessel emissions. When combined with the queuing stage effect, global emission display a broad-based reduction as a result of this new system.

Figure 7: Event Study (TWFE) - Voyage Emissions



3.3. Queuing Emission Effects

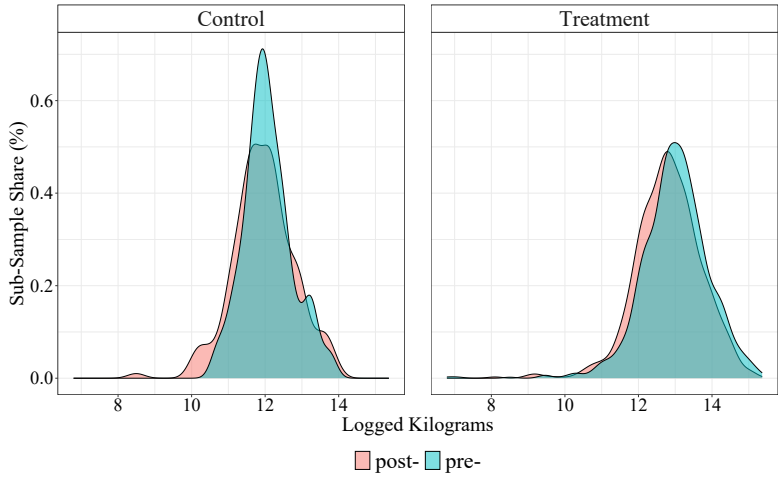
To represent the emissions of each vessel's queuing experience, I sum across emission contributions for a given ship on stage Q of transits and calculate three indicators; (i) total emissions, (ii) per nautical mile rate of emissions, and (iii) per hour rate of emissions. In Figure 8, I depict changes in emissions by treatment group and period. While there is a distinct reduction in queued vessel emissions among the treated group, the distribution of emissions among control vessels exhibits no directional drift (Figure 8a). The increased variance of the control group may be attributed to the particular drop in sample size for the period, as highlighted in Figure 8b.

I feature these adjustments in a difference-in-difference specification (Table 5) – sampling for vessels operating inbound from foreign origin ports and subject to no lane switching following the queue system's introduction. In Column 1, my findings suggest a 30.21% decline in vessel emissions during the queuing stage of transit. This evidence is supportive of the position that increased certainty of admittance timing, before arrival, encourages less loitering around the local port area.

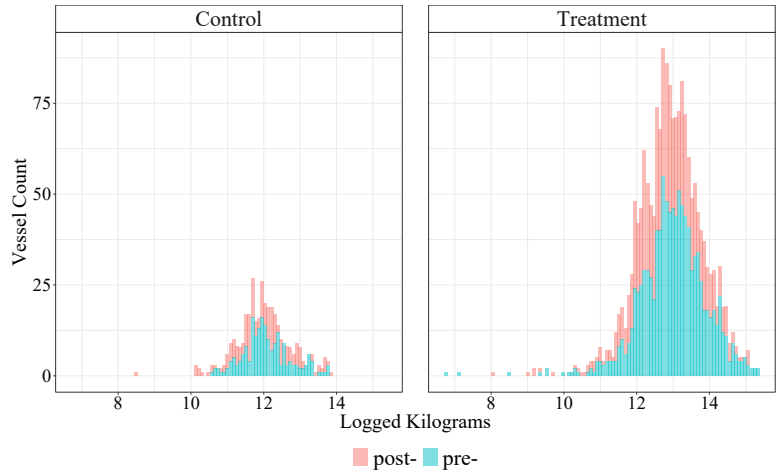
Breaking down the aspects of this overall result, the policy has contributed to a substantial reduction in time spent locally before port admittance – supportive of my proposed mechanism of greater certainty for arriving vessels enabling less time spent waiting. Since vessels are no longer idling as much and continuing to emit pollutants into the local area, emissions per nautical mile (knot) traveled decline (Column 3), and relatively more active vessels exhibit higher average travel speeds (Column 4). Columns (5) and (6) address potentially higher emissions resulting from increased exposure to the deep sea, and consequentially greater fuel consumption

Figure 8: CO_2 emissions by hour across queued vessels

(a) Distribution of Emissions by Subsample



(b) Number of Vessel-Voyages by Subsample



due to more frequent repositioning while waiting adrift offshore. These relatively less statistically significant findings highlight possible evidence that vessels were travelling slightly greater distances during their queuing stage, likely due to more frequent repositioning. Controlling for the shorter wait times, vessels' emissions per hour while queuing also rose by 11%, suggesting a greater degree of exertion following the blanket requirement to wait 150 nautical miles out at sea. Despite these demands though, it appears that improved certainty of queue positions outweighs the slightly worse waiting experience that vessels were exposed to.

Given these estimates, I next weigh the contributions of reduced voyage and

Table 5: Difference-in-Difference Estimates – Queuing Emissions

	CO_2 Emissions (1)	Duration (2)	Speed (3)	Em. per Knot (4)	Distance (5)	Em. per Hour (6)
Post–Period	-0.3114	-0.3302	0.0325	0.1116	-0.4231*	0.0187
	(0.2384)	(0.2663)	(0.1623)	(0.1685)	(0.2418)	(0.1068)
Treatment	1.299***	1.470***	-0.6342***	-0.4931**	1.792***	-0.1708
	(0.2067)	(0.2370)	(0.1051)	(0.2505)	(0.3774)	(0.1252)
DiD	-0.3021***	-0.4119***	0.4806***	-0.4508***	0.1487	0.1098*
	(0.0820)	(0.1183)	(0.0940)	(0.0871)	(0.1028)	(0.0658)
Vessel–Voyage FE	✓	✓	✓	✓	✓	✓
Year–Month FE	✓	✓	✓	✓	✓	✓
Observations	2,111	2,111	2,111	2,111	2,111	2,111
R^2	0.59	0.57	0.59	0.52	0.45	0.68

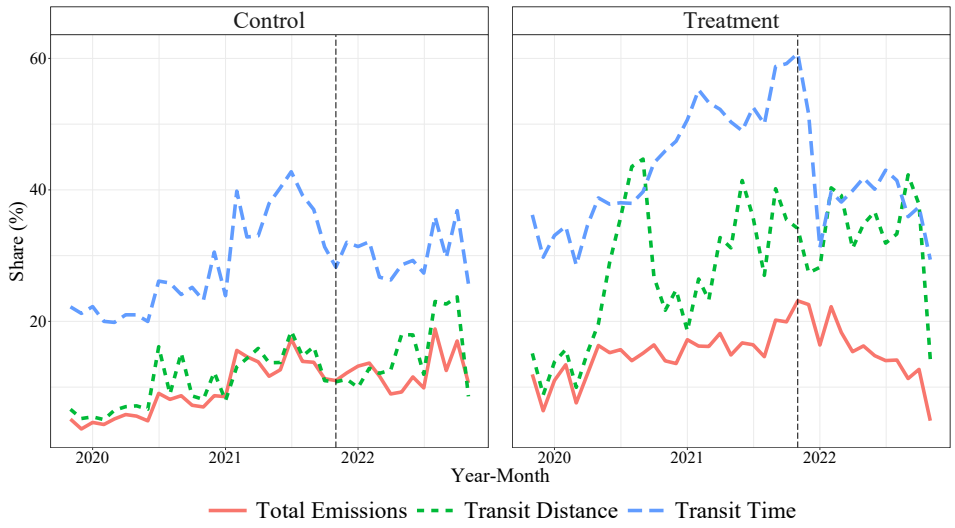
Note: ***: 0.01, **: 0.05, *: 0.1. Standard-errors are robust to clustering within vessel–voyage lanes of transport service. Each observation is a distinct queuing experience of a vessel arriving on the US west coast between Nov 2019 and Nov 2022. I filter only for vessel voyages that maintained the same international trade routes pre- and post-policy and drop any observations that lack matching vessel movement data. To limit extreme outlier distortions, I exclude any voyages with emissions less than the 25th percentile minus three times the interquartile range (75th percentile - 25th percentile) or higher than the 75th percentile plus three times the interquartile range (Davies and Jeppesen, 2015).

queuing emissions together and calculate the policy's overall global effect.

3.4. Global Emission Effects

In this section, I separately identify the voyage and queuing legs of a given vessel transit. As detailed in Figure 9, queuing represents a substantial share of the distance, duration, and associated emissions of international shipping.

Figure 9: Queuing Share of Global Containership Transit for US West Coast



Prior to the introduction of the new queuing system, both port groups experienced a doubling of vessel transit time allocated to the queuing experience across a two year time span. The introduction of ETA-based queue positions among treated ports – issued upon departure from a prior port of laden – was followed by a se-

vere decline transport operators' time allocated towards queuing. Unlike the control group, upward trends in the share of travel distance attributed to the queuing stage halted. Given the shorter durations vessels would remain within the port area, the queuing share of global emission contributions has also declined. Meanwhile, the control ports of Seattle, Tacoma and Oakland have largely maintained prior trends.

Referring to Equation 2, I assess the broad impact of the policy on global emissions by combining each vessels' voyage and queuing stages of transit. I find that the introduction of the new queuing system contributed to an 11.57% reduction in global vessel emissions servicing the US west coast.

Table 6: Difference-in-Difference Estimates – Global Emissions

	CO_2 Emissions (1)	Em. per Hour (2)	Em. per Knot (3)
Post–Period	-0.2081**	0.0891	-0.0954
	(0.0902)	(0.1103)	(0.0909)
Treatment	0.2084***	-0.1481	-0.1223
	(0.0744)	(0.1607)	(0.0865)
DiD	-0.1184***	-0.0372	-0.1560***
	(0.0447)	(0.0682)	(0.0481)
Vessel–Voyage FE	✓	✓	✓
Year–Month FE	✓	✓	✓
Observations	2,111	2,111	2,111
R^2	0.90	0.80	0.72

Note: ***: 0.01, **: 0.05, *: 0.1. Standard-errors are robust to clustering within vessel–voyage lanes of transport service. Each observation is a distinct global transit experience of a vessel arriving on the US west coast between Nov 2019 and Nov 2022. I filter only for vessel voyages that maintained the same international trade routes pre- and post- policy and drop any observations that lack matching vessel movement data. To limit extreme outlier distortions, I exclude any voyages with emissions less than the 25th percentile minus three times the interquartile range (75th percentile - 25th percentile) or higher than the 75th percentile plus three times the interquartile range (Davies and Jeppesen, 2015).

Furthermore, emissions per nautical mile traveled have declined by 15.88%. I do not detect a significant decline in emissions per hour due to increases during queuing offsetting reductions associated with voyage. While vessels have temporarily slowed down while at sea, the opposing effect of being more active during the queuing experience and potentially having to readjust position more frequently while waiting have added a partial upward effect to any broad adjustments in emissions per hour. In other words, vessels have repurposed available time that would have otherwise been allocated to the waiting & idling experience towards their voyages.

Although I identify a significant reduction in vessels' carbon emissions, primarily driven by strategic behaviour in the queuing leg of vessel voyages, this problem can also be approached indirectly. In the next section, I examine adjustments in local pollutants after introducing the new queuing system.

3.5. Commercial Port Activity

Although individual vessel-voyages have become more carbon efficient due to the new ETA-based queue system, the added certainty available to transport operators may yield additional effects that undermine local air quality. For example, should guaranteed queue positions be offered at a given port, this may present a better fit for 'just-in-time' production processes that many firms rely upon. As a result, this new system may also inadvertently attract more maritime commerce relative to other West Coast ports. Should the volume of transported goods outscale reductions in per vessels' contributions to local emissions, this policy may contribute towards an overall increase in emissions.

Table 7: Difference-in-Difference, Commercial Activity

Dep. Variable:	Trade (USD) (1)	Trade (KG) (2)	Loaded Containers (3)	Total Containers (4)
Post–Period	-0.1077	-0.1662	-0.2055***	-0.2146***
	(0.1596)	(0.1164)	(0.0459)	(0.0560)
Treatment	1.019***	0.7442***	1.041***	1.126***
	(0.0392)	(0.0312)	(0.0124)	(0.0123)
DiD	0.0864	0.1310*	0.1575***	0.2192***
	(0.0849)	(0.0674)	(0.0249)	(0.0253)
Month-Year FE	✓	✓	✓	✓
Observations	600	600	600	600
R^2	0.62	0.59	0.95	0.96

Note: ***: 0.01, **: 0.05, *: 0.1. White Standard-errors, robust to the presence of heteroskedasticity. Each observation is a year-month of containerized trade outcomes at the port level between January 2012 and June 2024. 'Post-Period' is equal to 1 for dates after November 2021. 'Treatment' is equal to 1 for ports of San Pedro Bay. The relevant control group consists of the ports of Oakland, Seattle, and Tacoma. Dependent variables are in log-form. 'Trade (USD)' represents the real value of containerized exports and imports, deflated using the St Louis FED's Consumer Price Index for All Urban Consumers: All Items Less Food and Energy in U.S. City Average. 'Trade (KG)' represents the total kilogram weight of containerized imports and exports. 'Loaded Containers' uses bilateral loaded container traffic flows reported directly by individual ports as a measure of market share/throughput. 'Total Containers' includes bilateral port flows of both loaded and empty containers.

In Table 7, I further exploit the quasi-natural experimental setting of this policy through a difference-in-difference approach to evaluate how various measures of commercial activity have varied, relative to the pre-period control ports of Seattle, Tacoma and Oakland. I find that commercial activity increased by approximately 8–23.5 percent, depending on whether goods or container flows are considered. Upon narrowing this evaluation to the COVID-period, pre- and post- policy, I find consistent results of a double-digit increase in commercial activity. Despite per vessel emissions falling locally, this policy has attracted greater flows of commercial activity to San Pedro Bay. This offsetting effect potentially lowers the gains I have documented for the local populace. In the next section, evaluate these factors jointly by exploring the direction that local emissions have shifted following the introduction

of San Pedro Bay's ETA-based queuing system.

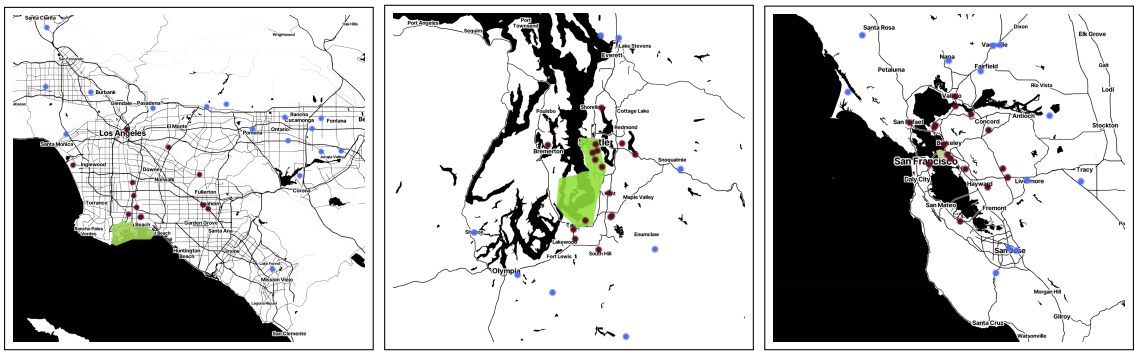
3.6. Local Air Quality

I adjust the difference-in-difference estimator to examine the system's effect on local air emissions, with treatment and control ports treated and non-treated US West Coast port areas. I estimate the policy effect on local emissions using the following specification:

$$Y_{ipt} = \alpha + \gamma_1 T_p + \gamma_2 D_t + \gamma_3 (T_p \times D_t) + \varepsilon_{ipt}, \tag{4}$$

where i identifies the monitor location, p indexes a given port region, t represents the associated date. Dummies T_p and D_t act as treatment and post-period dummies, respectively. T_p takes a value of 1 for any given coastal locations along Los Angeles and Long Beach, and is 0 otherwise.[12] D_t takes a value of 1 for any time period from November 11$^{\text{th}}$ 2021 onward. The dependent variable includes the following forms of emissions from AQI data; carbon monoxide (CO), sulfur oxides (SO_X), nitrogen oxide (NO_X), fine particulate matter ($PM_{2.5}$), and coarse particular matter (PM_{10}).

Figure 10: AQI Monitor Local Sites



Note: Each polygon depicts a port area. Red sites represent zone I monitors. Blue sites represent zone II monitors.

In Figure 10, I display Zone I – 'port-adjacent' monitors within 25 miles of the centroid of highlighted port areas – and Zone II – monitor groups between 25-50 miles from their respective port centroid.[13] I follow two specifications that alternate the key control group. For the initial set of results, the treatment (control) group

[12] To address concerns about vessel pollutants spreading across nearby coastal and inland regions of San Pedro Bay, I also compare against monitor sites of the non-treated set of port cities; Oakland, Seattle and Tacoma.

[13] Miles of distance between points are calculated using Vincenty distance, which accounts for the oblate spheroid curvature of the earth.

consists of monitors within 25 (between 25-50) miles of the San Pedro Bay port complex. In the second set of results, the treatment (control) group consists of monitors within 25 miles of the San Pedro Bay port complex (ports of Seattle or Oakland).

Upon reviewing the on-site effect, which compares zones I and II within San Pedro Bay, I find a significant increase in local emissions (Table 8). I find that the new system contributed positively to port-adjacent emissions through an approximate; (i) 10.9% increase in carbon monoxide, (ii) 12.1% rise in nitrogen dioxide, (iii) 11.2% rise in oxides of nitrogen, and (iv) 3.9% elevation in ozone levels.[14] Using particulate matter (PM) measures of pollutant concentrates, I find similar evidence of broad increases in emissions across monitors adjacent to the port area, relative to the outer zone of monitors (Table 9). PM_{10} emissions rose by a 23% and $PM_{2.5}$ rose by 5.4%. Sulfur emissions showed a slight decline, although not to a statistically significant extent.

Table 8: Difference-in-Difference, Control: San Pedro Bay, Zone-II

Dep. Variable:	CO (1)	NO2 (2)	NOx (3)	Ozone (4)
Post–Period	0.0976 (0.2539)	0.1382 (0.1670)	0.2977 (0.2551)	-0.2403 (0.1635)
Treated	0.0189 (0.0031)	-0.0392** (0.0014)	0.0819*** (0.0012)	-0.1824*** (0.0001)
DiD	0.1089** (0.0019)	0.1213*** (0.0015)	0.1121*** (0.0013)	0.0386*** (4.14×10^{-5})
Day FE Month-Year FE	✓ ✓	✓ ✓	✓ ✓	✓ ✓
Observations R^2	17,804 0.30	21,127 0.33	21,141 0.32	18,294 0.49

Note: ***: 0.01, **: 0.05, *: 0.1. Standard-errors are robust to clustering by monitor zone. Each observation is a distinct day-monitor-port emission type reading. 'Post-Period' is equal to 1 for dates November 11th 2021 to October 30th 2022. 'Treatment' is equal to 1 for air pollutant concentration monitors within a 25-mile radius (Zone I) of the centroid of the San Pedro Bay port complex. The relevant control group consists of monitors within 25-50 miles of the same reference point (Zone II).

In the second specification of this assessment, I contrast outcomes across port-adjacent monitors near the ports of Los Angeles and Long Beach to other port-adjacent monitors positioned along the West Coast (Table 10). This may address concerns that particular vessel emissions may struggle to permeate regions beyond 25 miles of the US coastline. Results are broadly supportive of findings in Table 8, both in terms of direction and relative magnitudes across emission types.

[14]These upward shifts are relative to adjacent inner-city monitor zones distanced between 25-50 miles from the San Pedro port area.

Table 9: Difference-in-Difference, Control: San Pedro Bay, Zone-II

Dep. Variable:	PM_{10} (1)	$PM_{10-2.5}$ (2)	$PM_{2.5}$ (3)	SO2 (4)
Post–Period	-0.1898*	0.2919	-0.3486	0.3764*
	(0.0160)	(0.0582)	(0.2103)	(0.0311)
Treated	-0.3151***	-0.5804***	0.0032	-0.4552*
	(0.0018)	(0.0035)	(0.0014)	(0.0370)
DiD	0.2302**	0.1582**	0.0541*	-0.0966
	(0.0052)	(0.0070)	(0.0045)	(0.0349)
Day FE	✓	✓	✓	✓
Year–Month FE	✓	✓	✓	✓
Observations	6,949	1,303	14,471	3,853
R^2	0.22	0.40	0.25	0.19

Note: ***: 0.01, **: 0.05, *: 0.1. Standard-errors are robust to clustering by monitor zone. Each observation is a distinct day-monitor-port emission type reading. 'Post-Period' is equal to 1 for dates November 11th 2021 to October 30th 2022. 'Treatment' is equal to 1 for air pollutant concentration monitors within a 25-mile radius (Zone I) of the centroid of the San Pedro Bay port complex. The relevant control group consists of monitors within 25-50 miles of the same reference point (Zone II).

Table 10: Difference-in-Difference, Control: Seattle/Oakland, Zone-I

Dep. Variable:	CO (1)	NO2 (2)	NOx (3)	Ozone (4)
Post–Period	0.3445**	0.3377**	0.5386**	-0.4985**
	(0.0639)	(0.0639)	(0.1071)	(0.0712)
Treated	-0.2141*	0.3427**	0.3074	0.2007***
	(0.0502)	(0.0579)	(0.1054)	(0.0078)
DiD	0.1577***	0.1085**	0.1864***	0.0402**
	(0.0078)	(0.0145)	(0.0019)	(0.0073)
Day FE	✓	✓	✓	✓
Year–Month FE	✓	✓	✓	✓
Observations	17,788	21,738	20,732	17,385
R^2	0.29	0.41	0.36	0.41

Note: ***: 0.01, **: 0.05, *: 0.1. Standard-errors are robust to clustering by monitor zone. Each observation is a distinct day-monitor-port emission type reading. 'Post-Period' is equal to 1 for dates November 11th 2021 to October 30th 2022. 'Treatment' is equal to 1 for air pollutant concentration monitors within a 25-mile radius (Zone I) of the centroid of the San Pedro Bay port complex. The relevant control group consists of monitors within 25 miles of the Port of Seattle and the Port of Oakland.

Referring to particulate matter emissions in Table 11, port-to-port difference-in-difference comparisons yield further evidence of a statistically significant rise in emissions upon the introduction of the new port queuing system. Notable deviations from the zone-based results listed in Table 9 include a near doubling of particulate matter between 2.5 and 10 micrometers in diameter. Additionally, a somewhat significant decline in sulfur dioxide is detected, a pollutant relatively more associated

with vessel emissions than other port assets. This further emphasizes that despite vessel contributions declining, increased commerce has contributed to an overall rise in emissions, relative to other West Coast regions.

Table 11: Difference-in-Difference, Control: Seattle/Oakland, Zone-I

Dep. Variable:	PM_{10} (1)	$PM_{10-2.5}$ (2)	$PM_{2.5}$ (3)	SO2 (4)
Post–Period	0.0164	-0.3332	0.4302	0.1943
	(0.2726)	(0.2562)	(0.3694)	(0.1447)
Treated	0.5940	1.426***	0.5539**	-0.2624**
	(0.2523)	(0.0051)	(0.1093)	(0.0510)
DiD	0.2863***	0.9336***	0.0107	-0.3240*
	(0.0264)	(0.0040)	(0.0113)	(0.1001)
Day FE	✓	✓	✓	✓
Year–Month FE	✓	✓	✓	✓
Observations	3,330	925	27,184	8,802
R^2	0.38	0.71	0.22	0.07

Note: ***: 0.01, **: 0.05, *: 0.1. Standard-errors are robust to clustering by monitor zone. Each observation is a distinct day-monitor-port emission type reading. 'Post-Period' is equal to 1 for dates November 11th 2021 to October 30th 2022. 'Treatment' is equal to 1 for air pollutant concentration monitors within a 25-mile radius (Zone I) of the centroid of the San Pedro Bay port complex. The relevant control group consists of monitors within 25 miles of the Port of Seattle and the Port of Oakland.

4. Discussion & Conclusion

This paper determines the environmental effects of an ETA-based vessel queuing system and uses the case study of San Pedro Bay to show that the emissivity of containership vessels declines when controlling for prevailing trends along the other major container ports of the US West Coast. These new conditions enabled transport operators to learn their queue position before arriving in the local port area. As a result, operators could strategically adjust speeds and minimize the amount of idling they would perform in the local port vicinity. This contributed to a 41.2% reduction in queue times at port and a 30.2% reduction in per-vessel local emissions.

Additionally, my findings suggest that the new queuing system encouraged a partial slowdown in vessels. Voyage emissions were reduced by approximately 10.71% and travel speeds fell by 19.44%. Coupled with the event study design of this analysis, I posit that these adjustments are transitive and those relative slowdowns across vessels became statistically insignificant in less than a year.

To document the relative importance of these two stages of transit, I combine the international and local effects of the new queuing system and assess global impli-

cations. Firstly, I document that despite the small geographic region that queuing is contained within, this activity represents a substantial share of the timespan of a given vessel–voyage. In duration, it can range between a 20–60% year–month average share of total international transit times between ports. In emissions and distance, year–month averages range from 5–40%. The queuing stage is therefore a very important aspect of containership voyages that carries great weight in efforts to mitigate emissions. Accounting for both legs of transit, I find that the new queuing system of San Pedro Bay is attributable to an 11.57% reduction in total vessel emissions. Vessels in fact speed up during the queuing stage, due to less idling. This combined with the temporary slowdown in voyage speeds leads to a muted effect on average emissions per hour. Despite this fact, a substantial reduction in wait times occurs, which has led to emissions per nautical mile traversed in service of San Pedro Bay falling by 15.88%.

However, local monitors adjacent to West Coast port regions show signs of a relative elevation in emissions among post-period treated ports. I attribute this overall degradation in air quality to increased commercial activity at Los Angeles and Long Beach, following the policy's success in relieving the local logjam in container movements and its ability to better conform with 'just-in-time' production networks. This is reflected through a relative increase in container handling of 23.51%. Coupled together, these findings suggest that an ETA-based queuing system offers a substantial decarbonization boon to ports exposed to lengthy wait time and queuing processes. For small or mid-tier ports less likely to exhibit lengthy idling times, further study is required to establish whether the logistical costs of maintaining an ETA-based queuing system would be environmentally beneficial. Furthermore, port authorties should anticipate their maritime carbon footprint falling while their overall footprint may rise. This may be especially true in isolated incidents of system changes, where local commerce from other ports is inadvertently absorbed and per-vessel emissions reductions are offset by increased container handling volumes.

References

Bai, C., Y. Li, B. Liu, Z. Zhang, and P. Wu (2020). Gaseous Emissions from a Seagoing Ship under Different Operating Conditions in the Coastal Region of China. *Atmosphere 11*(3).

Brancaccio, G., M. Kalouptsidi, and T. Papageorgiou (2020). Geography, transportation, and endogenous trade costs. *Econometrica 88*(2), 657–691.

Capaldo, K., J. J. Corbett, P. Kasibhatla, P. Fischbeck, and S. N. Pandis (1999). Effects of ship emissions on sulphur cycling and radiative climate forcing over the ocean. *Nature 400*(6746), 743–746.

Corbett, J. J., H. Wang, and J. J. Winebrake (2009). The effectiveness and costs of speed reductions on emissions from international shipping. *Transportation Research Part D: Transport and Environment 14*(8), 593–598.

Corbett, J. J., J. J. Winebrake, E. H. Green, P. Kasibhatla, V. Eyring, and A. Lauer (2007). Mortality from Ship Emissions: A Global Assessment. *Environmental Science and Technology 41*(24), 8512–8518. PMID: 18200887.

Cristea, A., D. Hummels, L. Puzzello, and M. Avetisyan (2013). Trade and the greenhouse gas emissions from international freight transport. *Journal of Environmental Economics and Management 65*(1), 153–173.

Czermański, E., G. T. Cirella, A. Oniszczuk-Jastrzabek, B. Pawłowska, and T. Notteboom (2021). An Energy Consumption Approach to Estimate Air Emission Reductions in Container Shipping. *Energies 14*(2).

Davies, R. and T. Jeppesen (2015). Export mode, firm heterogeneity, and source country characteristics. *Review of World Economics (Weltwirtschaftliches Archiv) 151*(2), 169–195.

Economides, P. (2024). Unconventional Protectionism in Containerized Shipping. In *Working Papers Set*.

Ganapati, S. and W. F. Wong (2023). How Far Goods Travel: Global Transport and Supply Chains from 1965–2020. *Journal of Economic Perspectives 37*(3), 3–30.

Gillingham, K. and P. Huang (2021). Racial Disparities in the Health Effects from Air Pollution: Evidence from Ports. NBER Working Papers 29108, National Bureau of Economic Research, Inc.

Hansen-Lewis, J. and M. M. Marcus (2022). Uncharted waters: Effects of maritime emission regulation. Technical report, National Bureau of Economic Research.

Heiland, I., A. Moxnes, K. H. Ulltveit-Moe, and Y. Zi (2019). Trade From Space: Shipping Networks and The Global Implications of Local Shocks. CEPR Discussion Papers 14193, C.E.P.R. Discussion Papers.

Hulskotte, J. and H. Denier van der Gon (2010). Fuel consumption and associated emissions from seagoing ships at berth derived from an on-board survey. *Atmospheric Environment 44*(9), 1229–1236.

IMO (2021). Fourth Greenhouse Gas Study 2020. Full report, International Maritime Organization.

Jalkanen, J.-P., L. Johansson, J. Kukkonen, A. Brink, J. Kalli, and T. Stipa (2012). Extension of an assessment model of ship traffic exhaust emissions for particulate matter and carbon monoxide. *Atmospheric Chemistry and Physics 12*(5), 2641–2659.

Ju, Y. and C. A. Hargreaves (2021). The impact of shipping co2 emissions from marine traffic in western singapore straits during covid-19. *Science of The Total Environment 789*, 148063.

Kinney, P. L., M. G. Gichuru, N. Volavka-Close, N. Ngo, P. K. Ndiba, A. Law, A. Gachanja, S. M. Gaita, S. N. Chillrud, and E. Sclar (2011). Traffic impacts on PM2.5 air quality in Nairobi, Kenya. *Environmental Science & Policy 14*(4), 369–378.

Klotz, R. and J. Berazneva (2022). Local Standards, Behavioral Adjustments, and Welfare: Evaluating California's Ocean-Going Vessel Fuel Rule. *Journal of the Association of Environmental and Resource Economists 9*(3), 383 – 424.

Liu, H., M. Fu, X. Jin, Y. Shang, D. Shindell, G. Faluvegi, C. Shindell, and K. He (2016, November). Health and climate impacts of ocean-going vessels in East Asia. *Nature Climate Change 6*(11), 1037–1041.

Lugovskyy, V., A. Skiba, and D. Terner (2023). Unintended Consequences of Environmental Regulation of Maritime Shipping: Carbon Leakage to Air Shipping. In *SSRN Electronic Journal*.

Mitchell, R. C. and R. Carson (1986). Property Rights, Protest, and the Siting of Hazardous Waste Facilities. *American Economic Review 76*(2), 285–90.

Molina, R., J. C. Villaseñor-Derbez, G. McDonald, and G. McDermott (2024). Dangerous Waters: The Economic Toll of Piracy on Maritime Shipping. CESifo Working Paper Series 11077, CESifo.

Morehouse, J. M. and E. A. Rubin (2021). Downwind and Out: The Strategic Dispersion of Power Plants and their Pollution. In *SSRN Electronic Journal*.

Ngo, N. S., M. Gatari, B. Yan, S. N. Chillrud, K. Bouhamam, and P. L. Kinney (2015). Occupational exposure to roadway emissions and inside informal settlements in sub-Saharan Africa: A pilot study in Nairobi, Kenya. *Atmospheric Environment 111*, 179–184.

Prochazka, V., R. Adland, and F.-C. Wolff (2019). Contracting decisions in the crude oil transportation market: Evidence from fixtures matched with AIS data. *Transportation Research Part A: Policy and Practice 130*(C), 37–53.

Rivera, N. (2021). Air quality warnings and temporary driving bans: Evidence from air pollution, car trips, and mass-transit ridership in Santiago. *Journal of Environmental Economics and Management 108*(C), S0095069621000371.

Rodrigue, J.-P. (2020, May). *The Geography of Transport Systems*. Fifth edition. — Abingdon, Oxon ; New York, NY : Routledge, 2020.: Routledge.

Schwarzkopf, D. A., R. Petrik, V. Matthias, M. Quante, E. Majamäki, and J.-P. Jalkanen (2021). A ship emission modeling system with scenario capabilities. *Atmospheric Environment: X 12*, 100132.

Scott, T. M. and F. Mayer (2023). International Trade, Noise Pollution, and Killer Whales. NBER Working Papers 31390, National Bureau of Economic Research, Inc.

Shapiro, J. (2016). Trade Costs, CO2, and the Environment. *American Economic Journal: Economic Policy 8*(4), 220–54.

Tumbarello, P., S. Arslanalp, and M. Marini (2019). Big Data on Vessel Traffic: Nowcasting Trade Flows in Real Time. IMF Working Papers 2019/275, International Monetary Fund.

Walsh, C. and A. Bows (2012). Size matters: Exploring the importance of vessel characteristics to inform estimates of shipping emissions. *Applied Energy 98*(C), 128–137.

Wong, W. F. (2022). The Round Trip Effect: Endogenous Transport Costs and International Trade. *American Economic Journal: Applied Economics 14*(4), 127–66.

Wong, W. F. and S. Fuchs (2022). Multimodal Transport Networks. FRB Atlanta Working Paper 2022-13, Federal Reserve Bank of Atlanta.

Zhang, Y., S. D. Eastham, A. K. Lau, J. C. Fung, and N. E. Selin (2021, aug). Global air quality and health impacts of domestic and international shipping. *Environmental Research Letters 16*(8), 084055.

Zou, E. Y. (2021). Unwatched Pollution: The Effect of Intermittent Monitoring on Air Quality. *American Economic Review 111*(7), 2101–26.

Appendix

I. Data Description

The construction of voyage data yields each individual vessel's associated emissions in lieu of arriving at a given port. These measures are constructed through many stages of cleaning with respect to vessel position data provided by MarineCadastre.

Port Statistical Areas (USACE)

I identify the top ports of containerized shipping based on Panjiva records of twenty-foot equivalent unit (TEU) container traffic.[15] i then access public records of port statistical areas, provided by the United States Army Corps of Engineers (USACE). I construct polygon areas manually for any missing ports, taking guidance from each ports provided facility maps. In cases where facility maps are not provided, I refer to satellite imagery provided by Google Earth. These port polygons are used to track the entry and exit of individual vessels, using their geolocations which are updated in minute intervals.

Matching MarineTraffic (MT) and MarineCadastre (MC)

MT provides records of port departure timestamps across vessels bound for the US West Coast. MC provides the individual micro-movements of uniquely identified vessels for the same time period in US waters. Using unique identifiers, the MMSI and IMO codes of each vessel, and the range of calendar dates between a prior departure and US West Coast arrival, I capture the initial moment each vessel enters US waters. For the subset of uniquely identified vessels that are not detected in US waters between these key dates, I label these vessels as "missing". The rate of missingness is relatively low, averaging less than 1 percent of the MT sample. However, I do detect a notable spike in missingness in 2020 for the months of July, August, and September. This appears to be largely concentrated among the ports of California.

Upon assembling a panel of data for individual vessel-voyages destined for the US West Coast, I merge vessel registry data made available on VesselTracking.net. This details the container capacity and build year of each vessel and allows me to validate whether the vessel IMO codes I have been provided match registered containerships. I extract a 100 percent match between issued vessels from MT to containerships registry records, which ensures I am not inadvertently including other vessel types in my analyses.

[15] See https://www.logisticsmgmt.com/article/top_30_u.s._ports_big_ports_got_bigger_in_2020

II. Fuel Consumption Function

Using Figure 4 from Rodrigue (2020), I digitalize each function into a set of coordinates, paired with the midpoint of ship size value based on the ranges displayed. I then generate an approximated function to represent each of these five functions, excluding "10,000+" for representing an undefined midpoint. Taking 1,000 equidistant grid points of speed (knots) between 0 and 25, I feed this range into each function and generate a dataframe of speeds (X), fuel consumption levels (Y), and container capacities (Z).

I regress the following specification of interacted and polynominal terms to estimate fuel consumption (Y), given a combination of speed (X) and TEU capacity values (Z).

$$Y_i = \alpha + \beta_1 X + \beta_2 Z_i + \beta_3 X_i^2 + \beta_4 Z_i^2 + \beta_5 X_i \times Z_i + \beta_6 X_i^2 \times Z_i + \varepsilon_i \tag{5}$$

Taking the set of estimated parameters $\{\hat{\alpha}, \hat{\beta}_1, \ldots, \hat{\beta}_6\}$, I use the resulting bivariate polynomial function to convert a given vessel's speed and container capacity into estimated fuel consumption. The resulting function is convex in speed and appears to rise non-linearly with increased to vessel mass. In Figure 11 below, I plot these estimates against the defined functions featured in 4 for select capacity ranges to better represent the appropriate fit this specification delivers. It should be highlighted that the function performs poorly at levels of speed less frequently observed in practice. In these extreme cases of slow speed, I refer to maritime transport estimates detailed in the next appendix subsection.

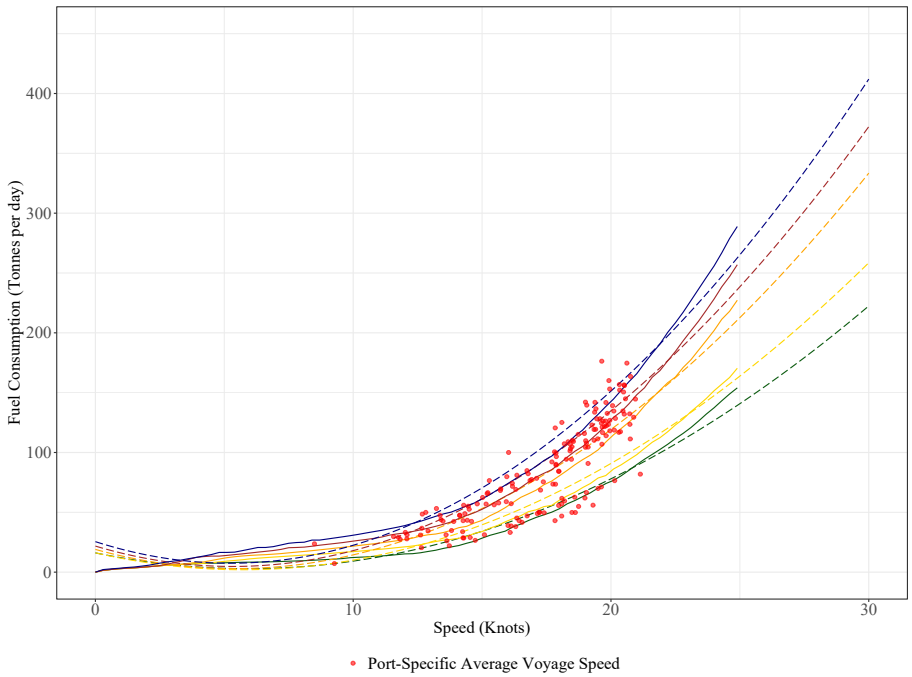
III. Queuing Emissions & Additional Findings

In this section, I provide further insight into how queuing emissions are summarised for individual vessel–voyages. Additionally, I provide supportive evidence of my main findings in which I broaden the sample of relevant vessels.

Local Queuing Emissions Calculations

I refer to Bai et al. (2020) to estimate fuel consumption associated with queuing activity – a combination of stationary and active movements, which includes cruising, maneuvering, and anchored stauses. This study decomposes time and speed across these various stages of local presence, and identifies associated emissions as

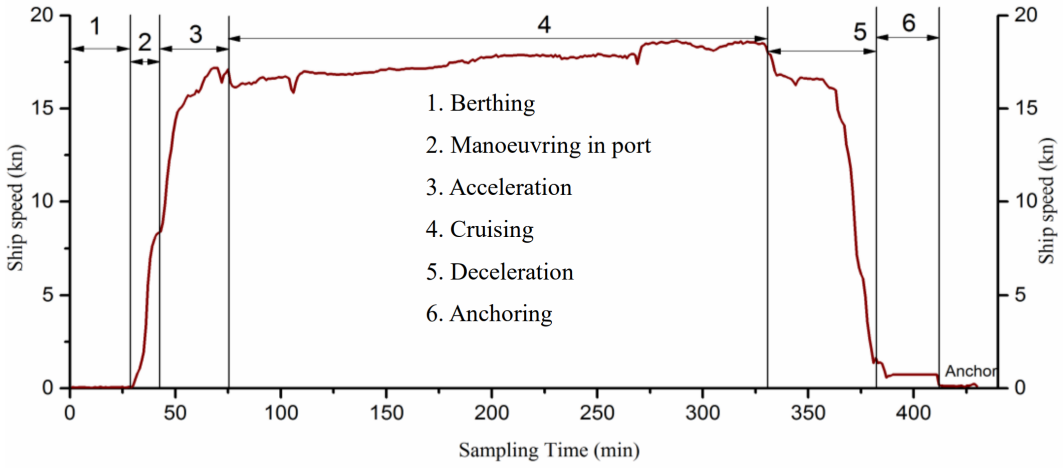
Figure 11: Fuel Consumption Function



Note: Dashed lines represent imputed functions with TEU fixed at the midpoint of ranges associated with solid line. Solid line functions were mapped using graph readers applied to figures featured in Rodrigue (2020).

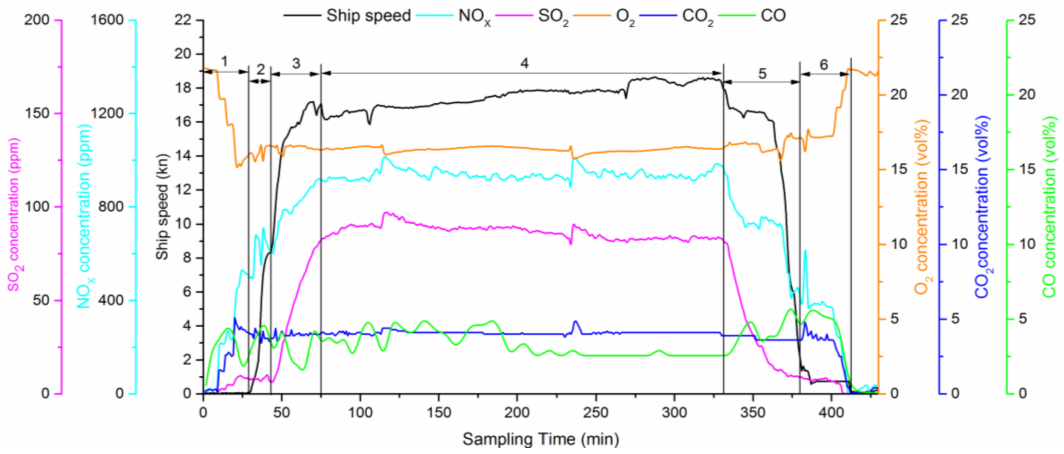
momentum of large vessels slowly accumulates from a stationary position. Figure 13 demonstrates how speed adjusts across difference stages of vessel transit. Figure 13 provides a depiction of the corresponding adjustments in emission types based on these stages and speeds within each stage.

Figure 12: Speed by Stage



Source: Bai et al. (2020), Gaseous Emissions from a Seagoing Ship under Different Operating Conditions in the Coastal Region of China, Atmosphere, Vol. 11(3), pp 305.

Figure 13: Emissions by Speed-Stage



Source: Bai et al. (2020), Gaseous Emissions from a Seagoing Ship under Different Operating Conditions in the Coastal Region of China, Atmosphere, Vol. 11(3), pp 305.

For a given series of local movements, I observe the travel speed S and container capacity C of each vessel within US waters at timestamp t. Timestamps are updated at a minute-level resolution and the previous observation's timestamp for vessel i corresponds to the earlier point of t'. The set of emissivity indices are represented by $(3206, 10.50, 50.50, 2.30)$, which assumes compliance with the IMO 2020 sulfur content mandate. For each reported position p of vessel i, I take the following steps.

If $S_{ipt} > 10$:

- Generate $\Phi_{ipt}\left(S_{ipt}, C_i\right)$ for fuel consumption in tonnes per day
- Measure $\Phi_{ipt}\left(S_{ipt}, C_i\right) * (\text{Emissivity Indices})$ as the kilograms rate of associated emissions per day
- Take timestamps t and $t-1$ to calculate $\gamma_{ipt}\left(t, t'\right) = \frac{t-t'}{24}$ to scale for the percentage of a day that has elapsed between two consecutive vessel coordinate pings
- Calculate $\delta_{ipt}(S_{ipt}, C_i, t, t') = \gamma_{ipt}\left(t, t'\right) \Phi_{ipt}\left(S_{ipt}, C_i\right) (\text{Emissivity Indices})$ to indicate the total kilogram emissions of vessel i between time t and t', for CO_2, SO_X, NO_X and $PM_{2.5}$, respectively

If $S_{ipt} \leq 10$, repeat the above steps with speed held fixed at 10 for fuel consumption, $\Phi_{ipt}\left(10, C_i\right)$. Upon multiplying by the appropriate emissivity index value, the total kilogram emissions contribution between t' and t is reduced by an emissions

scaling factor, based on slow travel speed pollutant levels mapped in Figure 13.[16]

DiD – All International Voyages

Rather than keeping vessel voyages on fixed lanes, I relax the sample to allow for vessels to adjust which origins they stem from following the introduction of the new queuing system. As displayed in Figure 12, I find strikingly similar results to those featured in Figure 5 across each of my indicators of local vessel activity and emissivity.

Table 12: Difference-in-Difference Estimates – Queuing Emissions

	Total Emissions (1)	Duration (2)	Speed (3)	Em. per Knot (4)	Distance (5)	Em. per Hour (6)
Post–Period	-0.4646**	-0.5030**	0.0733	0.1206	-0.5852**	0.0384
	(0.1969)	(0.2179)	(0.1507)	(0.1542)	(0.2306)	(0.0920)
Treatment	0.7243***	0.8548***	-0.4183***	-0.3460***	1.070***	-0.1305**
	(0.0970)	(0.1082)	(0.0746)	(0.0776)	(0.1296)	(0.0539)
DiD	-0.2125***	-0.2865***	0.3617***	-0.3787***	0.1662*	0.0741
	(0.0754)	(0.1000)	(0.0801)	(0.0755)	(0.0946)	(0.0563)
Vessel–Voyage FE	✓	✓	✓	✓	✓	✓
Year–Month FE	✓	✓	✓	✓	✓	✓
Observations	5,090	5,090	5,089	5,090	5,090	5,090
R^2	0.70	0.70	0.72	0.66	0.63	0.78

Note: ***: 0.01, **: 0.05, *: 0.1. Standard-errors are robust to clustering within vessel–voyage lanes of transport service. Each observation is a distinct queuing experience of a vessel arriving on the US west coast between Nov 2019 and Nov 2022. I filter only for vessel voyages that maintained international trade routes pre- and post- policy and drop any observations that lack matching vessel movement data. To limit extreme outlier distortions, I exclude any voyages with emissions less than the 25th percentile minus three times the interquartile range (75th percentile - 25th percentile) or higher than the 75th percentile plus three times the interquartile range (Davies and Jeppesen, 2015).

For static berth activity, I recommend the use of a scaling factor proposed by Hulskotte and Denier van der Gon (2010) which receive frequent use in the maritime logistics literature (Jalkanen et al., 2012; Ju and Hargreaves, 2021; Schwarzkopf et al., 2021). This is a linear function of the gross tonnage of vessels times the hours spent stationary (Table 13). For the purposes of this study, assessing voyage and queuing stages of transit, I do not include berthing activity in broader analysis.

[16] At a speed of zero, NO_X during the maneuvering stage is measured at a concentration of 450ppm (64.29% of 10 knot speed emissions). Plotting each knots per hour measure relative to their emission concentrate deviations from 700 (the 10 knot maximum) allows for the mapping of an increasing, concave emission scaling factor function of speed. This approach assumes that each emission type accumulates at the same diminishing marginal rate at maneuvering speeds between 0–10 knots per hour. The exact formula I estimate is $ESF = 64.28571 + 7.539686x - 0.3968257x^2$.

Table 13: Estimate of Fuel Consumption by GT-Dwell Hours

Type of ship	Fuel Consumption Rate (kg fuel/1000 GT h)	Average hotelling time at berth (hours)
Oil Tankers	19.3	28
Chemical and other tankers	17.5	24
Bulk Carriers	2.4	52
Containers	5.0	21
General Cargo	5.4	25
Ferries and RoRo	6.9	24
Reefers	24.6	31
Other	9.2	46

Source: Hulskotte and Denier van der Gon (2010). Fuel Consumption and Associated Emissions from Seagoing Ships at Berth Derived from Onboard Survey, Atmospheric Environment, Vol. 44(9), pp 1229–1236.